

Scale-Dependent Reproduction of Pen-and-Ink Illustrations

Mike Salisbury

Corin Anderson

Dani Lischinski

David H. Salesin

Department of Computer Science and Engineering
University of Washington

Abstract

This paper describes a representation for pen-and-ink illustrations that allows the creation of high-fidelity illustrations at any scale or resolution. We represent a pen-and-ink illustration as a low-resolution grey-scale image, augmented by a set of discontinuity segments, along with a stroke texture. To render an illustration at a particular scale, we first rescale the grey-scale image to the desired size and then hatch the resulting image with pen-and-ink strokes. The main technical contribution of the paper is a new reconstruction algorithm that magnifies the low-resolution image while keeping the resulting image sharp along discontinuities.

CR Categories and Subject Descriptors: I.3.3 [Computer Graphics]: Picture/Image Generation — Display algorithms; I.3.6 [Computer Graphics]: Methodology and Techniques — Device independence; I.4.3 [Image Processing]: Enhancement — Filtering.

Additional Key Words: discontinuity edges, image magnification, image resampling, non-photorealistic rendering, scale-dependent rendering, stroke textures.

1 Introduction

The medium of pen and ink offers many advantages for visually communicating ideas. Pen-and-ink illustrations can be easily printed alongside text, using the same ink on the same paper, without degradation. Moreover, good reproduction quality can be obtained on commonplace 300 or 600 dot-per-inch laser printers as well as on lower-resolution monochrome displays. Although pen-and-ink illustrations allow only monochromatic strokes of the pen, the resulting illustrations are often striking in their beauty and simplicity [11, 24].

While the areas of photorealistic rendering and paint systems have received considerable attention in the literature, creating pen-and-ink illustrations on a computer is a relatively new area. Recently, Winkenbach and Salesin [28] described an automated rendering system that produces pen-and-ink illustrations from 3D polyhedral architectural models. This system can render an illustration of a model at different scales and resolutions by applying procedural stroke textures to an analytic representation of the image. Concurrently, Salisbury *et al.* [23] proposed an interactive system that allows the

user to “paint” an image with prioritized stroke textures. This system is particularly useful for applying stroke textures to a scanned or synthetic image, effectively creating an “artistically-half-toned” monochrome version of the original. The user creates the pen-and-ink illustration on the screen, and the illustration is saved as a long list of Bézier strokes. One problem with this straightforward WYSIWYG approach is that illustrations represented in this manner cannot be reproduced at different scales or resolutions without significantly changing their overall appearance.

By way of example, consider the three illustrations shown in Figure 1. Figure 1(b) shows the original illustration at the size for which it was designed by the artist. If we wish to double the size of the illustration, we cannot merely scale it by a factor of two; such a scaling lightens the tone by spreading the same number of strokes over a larger area, as demonstrated by Figure 1(c). While this effect could be mitigated by thickening the strokes in the scaled-up version, the character of the illustration would be considerably altered. Conversely, scaling the illustration down darkens the tone as the density of strokes increases (Figure 1(a)). We would instead like our computer-generated illustrations to maintain both the thickness and density of their strokes when they are rescaled. Changing resolutions could also produce unwanted effects. For instance, all three illustrations in Figure 1 would look darker on a 300 dot-per-inch printer as they use strokes that are too thin for that resolution.

Another problem with storing illustrations as Bézier strokes is that the sheer number of strokes can make such a representation expensive to store, slow to transmit, and cumbersome to include in electronic documents. For example, the size of each illustration in Figure 1 is about one megabyte in PostScript [1].

In this paper, we extend the work of Salisbury *et al.* by proposing an alternative representation for pen-and-ink illustrations that is scale- and resolution-independent as well as compact. Instead of storing each of the individual strokes comprising an illustration, we keep an underlying grey-scale image for each stroke texture in the illustration along with a pointer to the stroke texture itself. To render the illustration at a particular scale and resolution, the grey-scale images are first rescaled and then hatched with strokes.

The proposed image-based representation is quite simple; however, maintaining true scale- and resolution-independence also requires solving an interesting related problem whose solution is not so straightforward. Since pen-and-ink illustrations hatch an image with strokes, they tend to be insensitive to fine texture detail. Thus it is often sufficient for the underlying grey-scale image to have a relatively low resolution. However, magnifying a low-resolution image for reproducing a large illustration on a high-resolution output device typically results in undesirable blurring of the hard edges, or *discontinuities*, in the image.

The question, then, is how to resample images while preserving certain discontinuity edges. In order to be able to produce crisp edges in illustrations at all possible output scales and resolutions, we need to maintain information about discontinuity edges in the underlying image and explicitly take these edges into account in the resampling process. In this paper, we describe a new resampling algo-

University of Washington, Box 352350, Seattle WA 98195-2350
{ salisbur | corin | danix | salesin }@cs.washington.edu



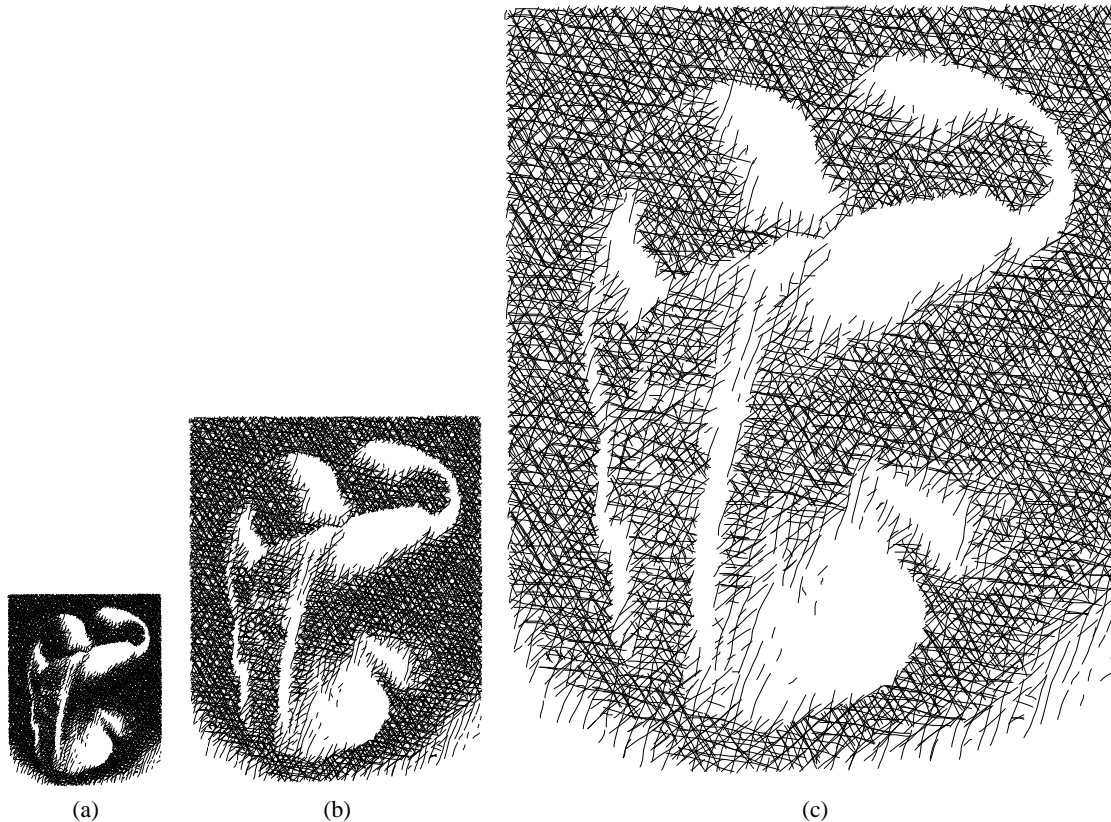


Figure 1 The same illustration at three different scales: (b) is the original; (a) and (c) demonstrate that naive rescaling changes tone and character.

rithm to implement this process. This algorithm, which is essentially a discontinuity-sensitive reconstruction filter, is the main technical contribution of the paper.

1.1 Related work

Line-art illustration has been explored previously by a number of authors. Elber [9], Saito and Takahashi [21], Winkenbach and Salesin [28], Strothotte *et al.* [25], and Lansdown and Schofield [14] all use 3D models to generate illustrations. Pnueli and Bruckstein [20] and Salisbury *et al.* [23] both generate illustrations starting from grey-scale images. However, neither of these last two works addresses the problem of rescaling such illustrations.

There are several paint systems that offer a measure of resolution-independence. Paint By Numbers [12] stores images as collections of resolution-independent strokes, Live Picture [16] represents the operations on images as a resolution-independent history, and Live-Paint [19] provides resolution-independent procedural ink. However, none of these approaches provides any means of magnifying scanned images beyond their original resolution while preserving discontinuities. The resampling algorithm described in this paper could conceivably be used for this purpose in any of these systems.

The idea of making explicit use of discontinuities in functions, surfaces, and images is not new. Discontinuities have been used to construct good meshes for radiosity [13, 15] and to fit piecewise-cubic interpolants for radiance functions [22]. Franke and Nielson described several methods for surface reconstruction from scattered data with known discontinuities [10]. Zhong and Mallat [31] pio-

neered work in image compression by storing edges detected at multiple scales. Yomdin and Elichai [30] also describe an image compression algorithm that locates and utilizes various types of edges in images to obtain a lossy compression scheme that avoids reconstruction artifacts in the vicinity of edges.

1.2 Overview

In the next section we describe in more detail our proposed representation scheme for pen-and-ink illustrations, and we present a new algorithm for image rescaling that preserves the discontinuities of the original image. Section 3 describes how pen-and-ink illustrations are created and reproduced in our illustration system. Section 4 presents several examples of illustrations and describes our experience with the proposed technique. We conclude and offer directions for further research in Section 5.

2 Reconstructing images with discontinuities

This section describes the core of our pen-and-ink illustration system: an image-based representation for illustrations, and a new reconstruction algorithm for resampling images with discontinuities.

We have two major requirements of our representation. First, it should allow us to produce pen-and-ink illustrations at any scale and resolution without changing the tone or character of the illustration. Second, the resulting illustrations must keep “sharp features” sharp and “smooth features” smooth. By “sharp features” we mean abrupt changes in intensity along certain prescribed boundaries of the im-

age, which we refer to as *discontinuities*. While we want our illustrations to exhibit crisp edges along discontinuities, we would like the tone to change smoothly everywhere else. In particular, it is important that the rescaling algorithm not introduce any spurious discontinuities.

One could imagine several possible representations that would meet our requirements. For example, we could maintain a history of all the operations performed on an image, along the lines of Live Picture [16], and then simply replay the history at the desired resolution when rendering the output. Although this approach is simple and basically sound, it has two main disadvantages. First, the representation's size and rendering time grow with the number of editing operations, and not necessarily with the complexity of the image. Second, this approach does not allow scanned or rendered images to be magnified beyond their original sizes without blurring their sharp features.

Another alternative is to use a collection of polynomial patches in order to construct an explicit image function that interpolates the image sample values. One difficulty with this representation is the problem of handling discontinuities, since it is not obvious how to modify a smooth patch representation to incorporate arbitrary arrangements of discontinuities. Another difficulty is the problem of determining control points so that the surface accurately approximates an arbitrary target image without introducing ringing artifacts from maintaining the smoothness constraints.

For our representation, we have chosen to use a combination of uniformly-spaced image samples and piecewise-linear discontinuity curves called *discontinuity edges*. Any arrangement of discontinuity edges is allowed, provided they intersect only at their endpoints. Thus, discontinuity edges are not constrained to form closed regions. Instead, we allow "open" discontinuities that have dangling edges not connected to any other. We would like the tone to change smoothly around the open end of such a discontinuity but change sharply across the discontinuity edge. It is crucial to allow open discontinuities, as they frequently arise in images, especially when discontinuity edges are obtained by performing edge detection on a scanned image (see Figure 6(b)).

In the rest of this section, we'll describe the algorithm we use to produce an image of arbitrary scale and resolution from our representation.

2.1 Problem statement

The problem that we would like to solve can be stated formally as follows:

Given: A set of uniformly-spaced discrete sample (pixel) locations $\{x_i\}$, a set of corresponding intensity values $\{f_i\}$, and a set of line segments $\{\ell_i\}$ (the discontinuity edges);

Find: A function $f(x)$ that is smooth everywhere except across the discontinuity edges, such that $f(x)$ interpolates the values f_i .

The reconstructed function $f(x)$ can then be resampled at a higher rate than the original image, resulting in a magnified version of the image, or it can be resampled at a lower rate after band-limiting, yielding a minified version of the image.

2.2 Reconstruction algorithm

Reconstruction of a continuous signal $f(x)$ from uniformly-spaced discrete samples $\{(x_i, f_i)\}$ may be performed by convolving with a reconstruction kernel $k(x)$, whose weights at the sample points sum to one:

$$f(x) = \sum f_i k(x - x_i). \quad (1)$$

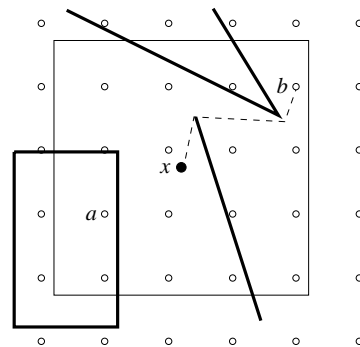


Figure 2 Several discontinuity edges (shown as thick lines) intersect the support of a 4×4 kernel centered at x . The dashed line indicates the shortest unobstructed path from x to b .

A variety of reconstruction kernels is available, including several interpolation kernels that effectively fit interpolants of various degrees to the input samples [29]. In this section, we describe a modification to the standard convolution framework that will cause the reconstructed function to be discontinuous across the discontinuity edges while preserving smoothness everywhere else.

In order to reconstruct the value at point x , we first check whether there are any discontinuity edges that cross the support of the kernel centered at x . If no such discontinuities exist, the reconstructed value $f(x)$ is given by equation (1).

Things become more interesting when one or more image samples under the kernel's support are separated from x by a discontinuity edge. Consider, for example, the situation in Figure 2. The thick solid lines indicate discontinuity edges that intersect the square support of the kernel centered at x (marked by a black dot). Input samples such as a cannot be reached from x without crossing a discontinuity edge. Clearly such samples should not have any effect on the value of $f(x)$. Input samples such as b cannot be "seen" directly from x ; however, they can be reached by going around the discontinuities. To ensure that $f(x)$ changes smoothly as x moves around these discontinuities, the sample b should have some effect on the value $f(x)$. Intuitively, this effect should be commensurate with the "ease" of reaching b from x without crossing discontinuities.

Thus, in order to preserve discontinuities in the reconstructed function $f(x)$, we replace the reconstruction kernel k with a modified kernel \tilde{k} , which attenuates k 's entries according to each entry's reachability. To describe our new kernel, we must first define some terms.

Let $d(x, x_i)$ be the Euclidean distance between x and x_i , and let $sp(x, x_i)$ be the length of the shortest unobstructed path between the two points (see Figure 2). We define the *detour cost* between x and x_i as:

$$detour(x, x_i) = sp(x, x_i) - d(x, x_i) \quad (2)$$

Our modified kernel \tilde{k} thus attenuates k :

$$\tilde{k}(x - x_i) = \alpha(x, x_i) k(x - x_i) \quad (3)$$

where the attenuating function $\alpha(x, x_i)$ is defined as:

$$\alpha(x, x_i) = \begin{cases} 1 & \text{if } detour(x, x_i) = 0 \\ & \text{(i.e., if } x_i \text{ is visible from } x) \\ 0 & \text{if } detour(x, x_i) \geq r \\ & \text{(i.e., if } x_i \text{ is too "far")} \\ 1 - 3t^2 + 2t^3 & \text{if } detour(x, x_i) < r, \\ & \text{where } t = detour(x, x_i)/r \end{cases} \quad (4)$$

The constant r above is the detour cost beyond which a sample has no effect on x . We have found that a value of $r = 1$ works well for

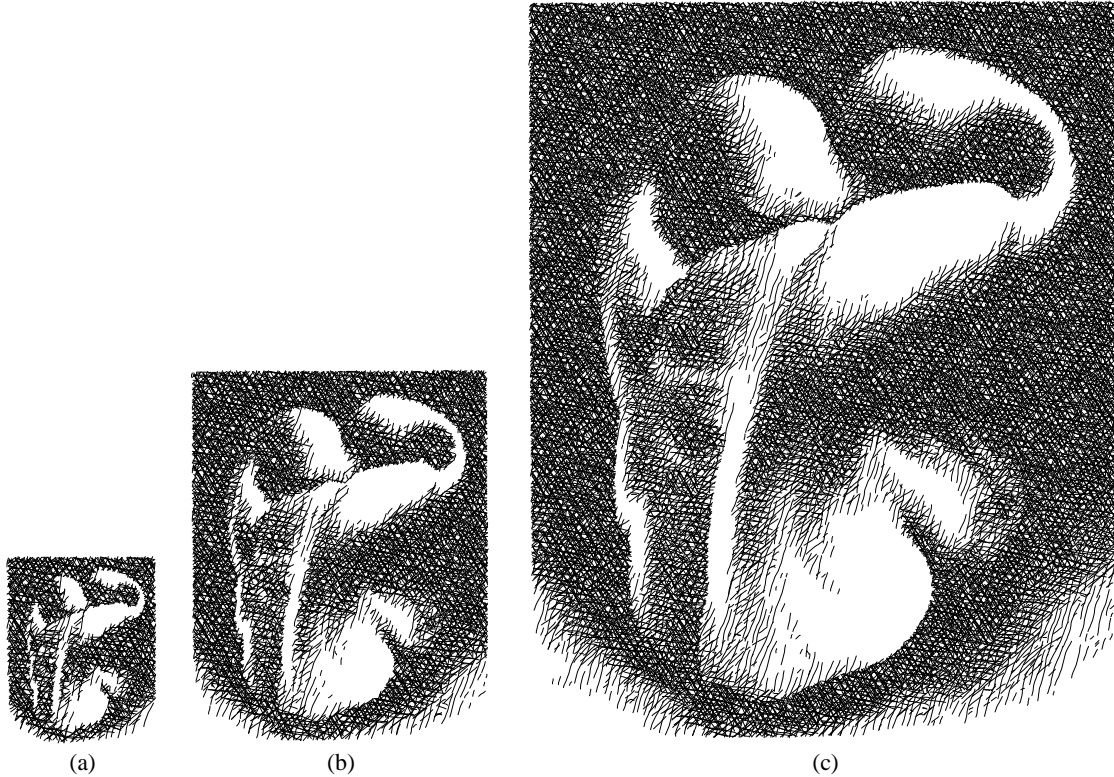


Figure 3 A pepper at three different scales. Original photograph by Edward Weston [27].

our 4×4 filter. The cubic polynomial in the third case above was chosen in order to ensure that $\alpha(x, x_i)$ is C^1 continuous.

Note that the modified kernel \tilde{k} no longer has the property that its weights at the sample points sum to one. To compensate, we turn the convolution in equation (1) into a *weighted-average* convolution:

$$f(x) = \frac{\sum f_i \alpha(x, x_i) k(x - x_i)}{\sum \alpha(x, x_i) k(x - x_i)} \quad (5)$$

This form of convolution has been used previously for filtering non-uniform samples [7, 8, 18].

The kernel modification described above is applicable to any reconstruction kernel. In our implementation, we chose the cubic convolution kernel described by Wolberg [29]. This kernel has negative lobes, as do most interpolating kernels. This property introduces a slight complication into our reconstruction algorithm, as it is possible for the magnitude of the sum in the denominator of equation (5) to become very small. Dividing by small numbers magnifies any noise in the calculation, causing visible bright “speckles” in the reconstructed image. To overcome this difficulty, we switch to the entirely non-negative B-spline kernel [29] whenever the denominator in equation (5) falls below a certain threshold. To avoid introducing a discontinuity at places where the switch occurs, we smoothly blend between the two kernels as the denominator approaches zero. A precise definition of these two kernels is given in Appendix A.

Our resampling algorithm resembles the “distance penalty fault” method described by Franke and Nielson for surface reconstruction from scattered data with known discontinuities [10]. However, our algorithm is specialized to uniform grid data, and by using the general notion of detour cost it can handle arbitrary arrangements of discontinuity edges. Another difference is that, unlike Franke and Nielson’s algorithm, ours is not restricted to positive weighting func-

tions, allowing better frequency response.

Computing shortest paths

To complete the description of our reconstruction algorithm, it remains to explain how we compute the length of the shortest path between two points. We will refer to an endpoint of a discontinuity edge as a *discontinuity vertex*. If a discontinuity vertex is in the middle of a chain of discontinuity edges and is thus reachable from multiple sides, we consider each side of the vertex to be a distinct discontinuity vertex for the purposes of this minimum distance algorithm. As a preprocessing step, we compute the distance between all pairs of discontinuity vertices using Dijkstra’s all-pairs shortest paths algorithm [2]. Then, during reconstruction, to compute the shortest path between two particular points x_1 and x_2 that cannot “see” each other, we find the sets V_1 and V_2 of discontinuity vertices directly visible to x_1 and x_2 , respectively, within a certain ellipse that surrounds them both. This ellipse has foci at x_1 and x_2 and contains all points x such that

$$d(x, x_1) + d(x, x_2) \leq d(x_1, x_2) + r \quad (6)$$

Any discontinuity vertex beyond this distance would make the detour cost larger than the maximum detour cost r , thereby forcing the sample’s attenuation $\alpha(x, x_i)$ to zero.

Given the sets V_1 and V_2 , the length of the shortest path between points x_1 and x_2 is simply

$$sp(x_1, x_2) = \min_{v_1 \in V_1, v_2 \in V_2} \{d(x_1, v_1) + sp(v_1, v_2) + d(v_2, x_2)\} \quad (7)$$

In order to rapidly determine the set V for any point x we first construct a constrained Delaunay triangulation (CDT) [6] containing

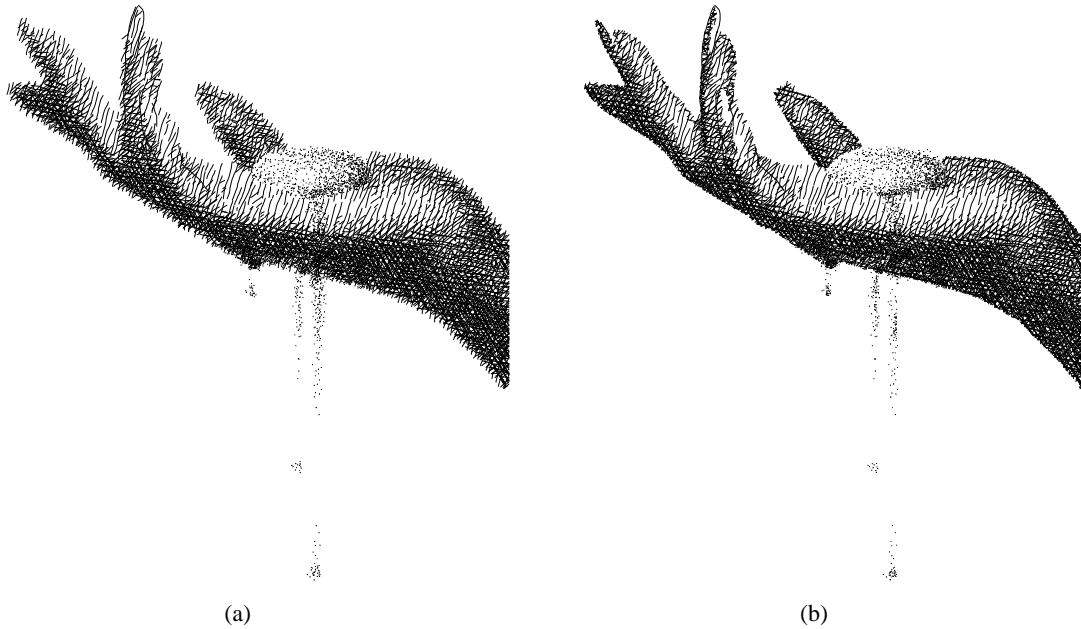


Figure 4 An illustration with standard filtering (a) and with our algorithm (b). Both illustrations were produced from images of the same resolution. Original photograph by Walter Swarthout [26].

all of the discontinuity edges in the image as a preprocessing step. Then, given the point x we locate the CDT face containing x . Starting from this face, we recursively visit all nearby faces that are reachable without crossing discontinuity edges. The vertices of all visited faces are tested to see if they are visible from x . To test the visibility of vertex v , we march from x towards v in the CDT and stop either when a discontinuity edge is crossed (in which case v is not directly visible), or when v is reached (in which case it is visible).

It costs $O(n^3)$ to compute the shortest paths between all pairs of n discontinuity edge vertices. The CDT can be constructed in $O(n \log n)$ time. Both of these computations are performed only once, in the preprocessing stage. For each point x at which the function is reconstructed (i.e., for each pixel location in the resampled image), we need to compute the detour cost for as many as sixteen pixels in the original image, as described above. The cost of this computation is at worst quadratic in the number of discontinuity vertices within the kernel’s support, but this number is typically small.

3 Creating and reproducing illustrations

Our illustration representation consists of a list of discontinuity edges and a grid of grey-scale sample values.

To create an illustration, we start from a grey-scale image. This image can be generated by rendering, digitally painting, or scanning in a printed image. We find discontinuity edges using Canny’s edge detector [5]. Then we compute one sample value at each pixel center. For most pixels, the source image pixel value is a good approximation to the sample value. However, for pixels containing discontinuities, the pixel value typically corresponds to an average of the image function on both sides of the discontinuity and is thus unsuitable as a sample value. In this case we extrapolate the sample value from nearby “uncontaminated” samples that are reachable without crossing discontinuities.

Once this process is completed, we reduce the resolution of the sample grid as much as possible while maintaining enough detail to

create a satisfactory result. If too few samples remain, some areas bounded by discontinuities may not contain any reachable sample values. In this situation we must allow the reconstruction filter to cross discontinuities. Thus, reducing the resolution too much may have the effect of blurring or eliminating small features altogether, even if their edges are part of the representation. Determining the appropriate reduction factor automatically is an interesting problem for future work.

Once the image has been reduced, we assign to it a stroke texture along with an optional set of *outline strokes* used to surround selected regions of the image. The outline strokes can be chosen from the set of discontinuity edges. To make use of multiple stroke textures, the image can be separated into grey-scale overlays, each of which is associated with its own stroke texture.

In order to view or print an illustration, we first produce a grey-scale image of the desired size with the algorithm described in Section 2. Since we want to avoid unnaturally sharp edges in the final illustration, we only magnify the image to one half of the desired size with our reconstruction algorithm. We then expand the image by an additional factor of two using a standard separable reconstruction filter, which can be applied much more quickly in a separate stage. This technique generates just enough blurring along the edges to give the illustrations a hand-drawn feel.

We finally re-render the illustration with a stroke texture in an automatic process called *blasting*. The blasting algorithm takes a grey-scale image and a stroke texture as input and creates an illustration with strokes, which, when taken together, produce the same tone as was present in the underlying image. We use the same approach as Salisbury *et al.* [23] for producing strokes and placing them into an illustration. This approach consists of repeatedly selecting a stroke from the stroke texture and computing the tone in the vicinity of the stroke that would result if it were added. The stroke is rejected if it makes the illustration darker than the tone of the underlying image anywhere along its length. Whereas the system of Salisbury *et al.* generates candidate strokes only underneath the user’s brush, we automatically place strokes that cover the entire illustration.



Figure 5 Keys. Original photograph by Randy Miller [17].

4 Results

We present several illustrations that demonstrate the various capabilities of our representation.

Figure 3 shows an illustration rendered at three scales. Each of these scales maintains the correct tone and gives the same overall texture effect. Note that different collections of actual strokes were used to generate the illustration at the various sizes. Compare these illustrations to those in Figure 1, where the same set of strokes was used for each scale, resulting in undesirable alterations in tone and overall effect.

Figure 4 demonstrates the advantage of maintaining and respecting discontinuities. Figure 4(a) is an illustration produced by blasting an image that was rescaled without maintaining discontinuities. The illustration in 4(b) is the same as 4(a) except that it was rescaled using our magnification algorithm. Notice that the outline edges do not align with the edges of the fingers in illustration 4(a). Also of interest is the use of multiple textures in both Figures 4 and 5.

The illustrations in Figures 6 and 7 are close-ups of the lower-right-hand corner of Figure 5 and show the potential for using our representation to generate poster-sized illustrations. Figure 6(a) shows the pixel values stored by the representation, which along with the discontinuity edges in 6(b) can be used to generate 6(d) and, in turn, 7(b). The images in 6(c) and 6(d) are the grey-scale images that were used to blast the illustrations in 7(a) and 7(b). All of the edges in these and the other illustrations we present were found automatically with our edge detector.

Notice in Figure 6(b) that the key is not completely surrounded by edges. In places where no discontinuity edges are present, our reconstruction produces smooth changes in grey-scale, even in the vicinity of discontinuity endpoints.

Table 1 gives the storage requirements and reconstruction times required for the illustrations in this paper. The REPRESENTATION column gives the number of pixels stored on disk, the number of discontinuities used, and the total size of both in kilobytes. The OUTPUT column gives the size of the reconstructed grey-scale image that

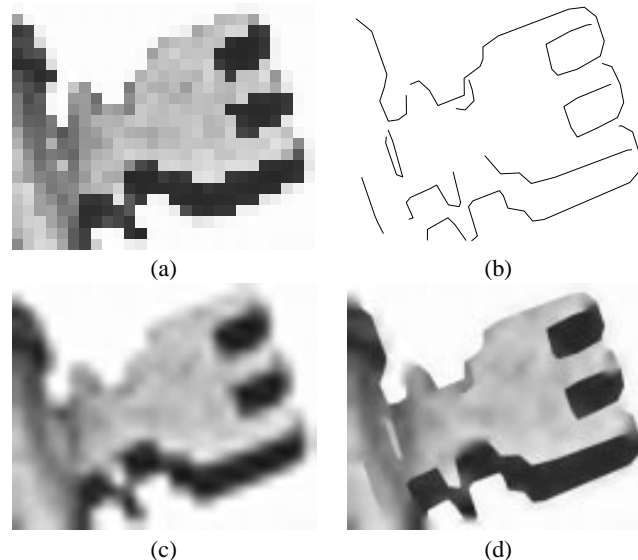


Figure 6 Close-ups of Figure 5: (a) the underlying low-resolution grey-scale image; (b) the discontinuity edges used; (c) the grey-scale image produced using standard magnification; and (d) the image produced by our resampling algorithm.

was used for blasting, and the size, in megabytes, of the PostScript file used for printing. Finally, the TIME column gives the time required to pre-process, enlarge, and blast the image with strokes. These times were measured on a Silicon Graphics workstation with a 250MHz R4400 processor. To summarize the table, our representation reduces the storage requirements of these illustrations by a factor of 100–1000, and it takes from 1–7 minutes to render them.

5 Future work

Our experience with the proposed technique suggests several areas for future research:

- *PostScript renderer.* The reduced size of our representation currently offers no practical advantage in transmission to printers or web browsers because they do not recognize our representation. One solution is to write rendering code in the languages that these devices do understand. For example, a PostScript printer could be sent illustration rendering code written in PostScript along with several standard stroke textures. This code could then generate an illustration at any requested scale and resolution directly on the output device. Similar programs could be written in Java or Acrobat to allow web browsers to render illustrations.
- *Scalable textures.* Currently our stroke textures are applied at a single scale: if the illustration is magnified, the texture shrinks relative to the image. While this effect is acceptable for uniform textures, it could be objectionable for textures with recognizable patterns. It might be better to have a multiresolution stroke texture that could change scale with the illustration. Then, as the scale of the texture increased, finer resolution strokes could automatically be added to the illustration.
- *Combining with multiresolution images.* Our representation and resampling algorithm are currently limited to traditional uniresolution images. We would like to extend our technique to handle multiresolution image representations, such as the one described by Berman *et al.* [4]. In this case, we would also want to develop

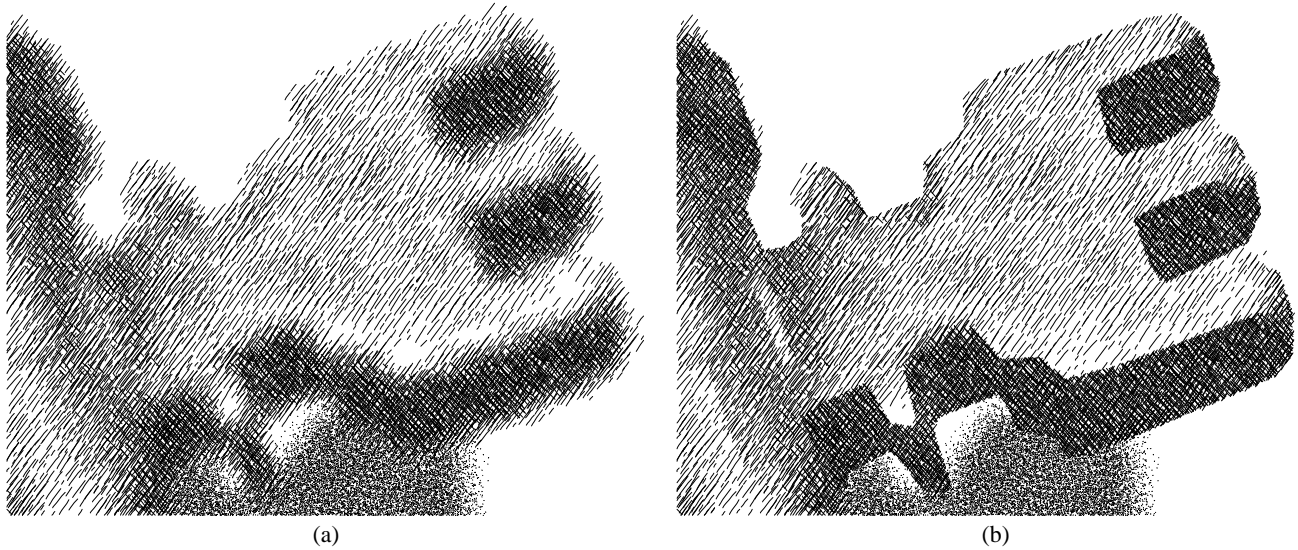


Figure 7 Illustrations produced from Figures 6(c) and 6(d).

Fig	Content	REPRESENTATION			OUTPUT		TIME		
		ImgSize (pixels)	# Edges	Storage (KB)	ImgSize (pixels)	PS Size (MB)	PreProc (sec)	Enlarge (sec)	Blast (sec)
3a	Pepper	102×128	270	10.5	204×256	0.2	39	3	5
3b	Pepper	102×128	270	10.5	408×512	1.0	39	35	11
3c	Pepper	102×128	270	10.5	816×1024	3.8	39	108	35
4a	Hand	64×64	—	1.2	1024×1024	1.0	—	3	45
"	Egg	128×128	—	1.4	1024×1024	1.0	—	4	128
4b	Hand	64×64	237	2.3	1024×1024	1.0	19	130	41
"	Egg	128×128	143	1.9	1024×1024	1.0	8	41	134
5	Keys	128×128	504	7.9	1024×1024	2.4	220	142	43
"	Shadow	64×64	111	1.5	1024×1024	2.4	3	100	120
7a	Key closeup	27×22	—	0.7	864×704	1.9	—	2	29
"	Shadow	27×22	—	0.2	864×704	1.9	—	2	88
7b	Key closeup	27×22	107	1.0	864×704	2.0	8	195	27
"	Shadow	27×22	6	0.3	864×704	2.0	1	30	84
8	Billiard	71×61	326	5.4	568×488	1.3	47	81	19

Table 1 Illustration sizes and speeds.

a multiresolution discontinuity representation in which different discontinuities could be present at different scales.

- *Image compression.* Given our algorithm's ability to reproduce large images from a compact representation, it is natural to consider the possibility of using it as a more general image compression mechanism. One complication with such an approach may be the lack of texture detail in the reconstructed images.

Acknowledgments

We would like to thank Sean Anderson for his help early in the project.

This work was supported by an Alfred P. Sloan Research Fellowship (BR-3495), an NSF Postdoctoral Research Associates in Experimental Sciences award (CDA-9404959), an NSF Presidential Faculty Fellow award (CCR-9553199), an ONR Young Investigator award (N00014-95-1-0728), a grant from the Washington Technology Center, and industrial gifts from Interval, Microsoft, and Xerox.

References

- [1] Adobe Systems Incorporated. *PostScript Language Reference Manual*. Addison Wesley, Reading, Massachusetts, 2nd edition, 1994.
- [2] Alfred V. Aho, John E. Hopcroft, and Jeffrey D. Ullman. *Data Structures and Algorithms*. Addison-Wesley, Reading, Massachusetts, 1987.
- [3] Arthur Beck. Photograph. In *Photographis 81, The International Annual of Advertising and Editorial Photography*, p. 151. Graphis Press Corp., 1981.
- [4] Deborah F. Berman, Jason T. Bartell, and David H. Salesin. Multiresolution painting and compositing. In *Computer Graphics Proceedings, Annual Conference Series*, pp. 85–90. ACM Press, July 1994.
- [5] John Canny. A computational approach to edge detection. *IEEE Transactions on Pattern Analysis and Machine Intelligence*, 8(6):679–698, November 1986.
- [6] L. Paul Chew. Constrained delaunay triangulations. *Algorithmica*, 4:97–108, 1989.
- [7] Robert L. Cook. Stochastic sampling in computer graphics. *Transactions on Graphics*, 5(1):51–72, January 1986.
- [8] Mark A. Z. Dippé and Erling Henry Wold. Antialiasing through stochastic sampling. *Computer Graphics*, 19(3):69–78, July 1985.

- [9] Gershon Elber. Line art rendering via a coverage of isoparametric curves. *IEEE Transactions on Visualization and Computer Graphics*, 1(3):231–239, September 1995.
- [10] Richard Franke and Gregory M. Nielson. Surface approximation with imposed conditions. In R. E. Barnhill and W. Boehm, editors, *Surfaces in CAGD*, pp. 135–146. North-Holland Publishing Company, 1983.
- [11] Arthur L. Guttill. *Rendering in Pen and Ink*. Watson-Guttill Publications, New York, 1976.
- [12] Paul E. Haeberli. Paint by numbers: Abstract image representations. *Computer Graphics*, 24(4):207–214, August 1990.
- [13] Paul Heckbert. Discontinuity meshing for radiosity. In *Third Eurographics Workshop on Rendering*, pp. 203–226, Bristol, UK, May 1992.
- [14] John Lansdown and Simon Schofield. Expressive rendering: A review of nonphotorealistic techniques. *IEEE Computer Graphics and Applications*, 15(3):29–37, May 1995.
- [15] Dani Lischinski, Filippo Tampieri, and Donald P. Greenberg. Discontinuity meshing for accurate radiosity. *IEEE Computer Graphics and Applications*, 12(6):25–39, November 1992.
- [16] T. Marshall. Lively pictures (Power Mac image editing). *BYTE*, 20(1):171–172, January 95.
- [17] Randy Miller. Photograph. In *Photographis 77, The International Annual of Advertising and Editorial Photography*, p. 72. Graphis Press Corp., 1977.
- [18] Don P. Mitchell. Generating antialiased images at low sampling densities. *Computer Graphics*, 21(4):65–72, July 1987.
- [19] Ken Perlin and Luiz Velho. Live Paint: painting with procedural multiscale textures. In *Computer Graphics Proceedings, Annual Conference Series*, pp. 153–160. ACM Press, August 1995.
- [20] Yachin Pnueli and Alfred M. Bruckstein. **DigⁱDürer** — a digital engraving system. *The Visual Computer*, 10(5):277–292, 1994.
- [21] Takafumi Saito and Tokiichiro Takahashi. NC machining with G-buffer method. *Computer Graphics*, 25(4):207–216, July 1991.
- [22] David Salesin, Daniel Lischinski, and Tony DeRose. Reconstructing illumination functions with selected discontinuities. In *Third Eurographics Workshop on Rendering*, pp. 99–112, Bristol, UK, May 1992.
- [23] Michael P. Salisbury, Sean E. Anderson, Ronen Barzel, and David H. Salesin. Interactive pen-and-ink illustration. In *Computer Graphics Proceedings, Annual Conference Series*, pp. 101–108. ACM Press, July 1994.
- [24] Gary Simmons. *The Technical Pen*. Watson-Guttill Publications, New York, 1992.
- [25] Thomas Strothotte, Bernhard Preim, Andreas Raab, Jutta Schumann, and David R. Forsey. How to render frames and influence people. *Computer Graphics Forum*, 13(3):455–466, 1994. Eurographics '94 Conference issue.
- [26] Walter Swarthout. Photograph. In *Photographis 75, The International Annual of Advertising, Editorial, and Television Photography*, p. 133. Graphis Press Corp., 1975.
- [27] Edward Weston. *Aperture Masters of Photography, Number Seven*, p. 29. Aperture Foundation, Inc., New York, 1988.
- [28] Georges Winkenbach and David H. Salesin. Computer-generated pen-and-ink illustration. In *Computer Graphics Proceedings, Annual Conference Series*, pp. 91–100. ACM Press, July 1994.
- [29] George Wolberg. *Digital Image Warping*. IEEE Computer Society Press, Los Alamitos, California, 1990.
- [30] Y. Yomdin and Y. Elichai. Normal forms representation: a technology for image compression. In *Image and Video Processing*, volume 1903 of *Proceedings of the SPIE — The International Society for Optical Engineering*, pp. 204–214. SPIE, February 1993.
- [31] S. Zhong and S. Mallat. Compact image representation from multi-scale edges. In *Proceedings, Third International Conference on Computer Vision*, pp. 522–525. IEEE Computing Society Press, December 1990.

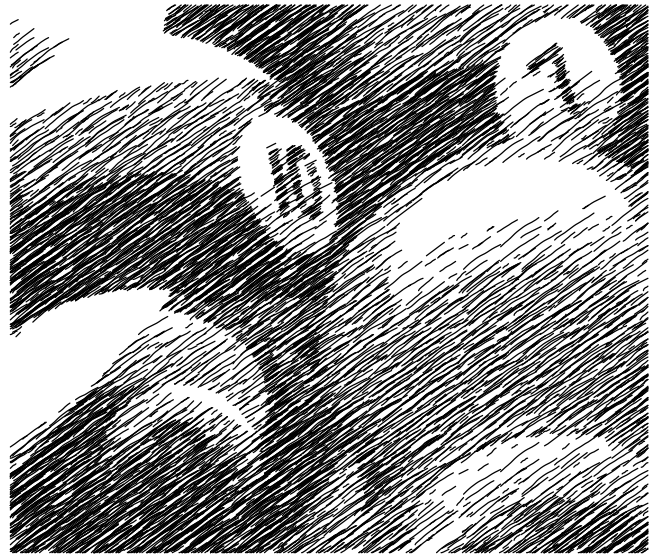


Figure 8 Billiard balls. Original photograph by Arthur Beck [3].

Appendix A: Kernel definitions

The cubic convolution kernel we used is a member of the following family of kernels [29]:

$$k(x) = \begin{cases} (a+2)|x|^3 - (a+3)|x|^2 + 1 & 0 \leq |x| < 1 \\ a|x|^3 - 5a|x|^2 + 8a|x| - 4a & 1 \leq |x| < 2 \\ 0 & 2 \leq |x| \end{cases} \quad (8)$$

We chose the value $a = -0.5$, which makes the Taylor series approximation of the reconstructed function agree in as many terms as possible with the original signal.

The non-negative B-spline kernel we used is defined as follows:

$$k(x) = \frac{1}{6} \begin{cases} 3|x|^3 - 6|x|^2 + 4 & 0 \leq |x| < 1 \\ -|x|^3 + 6|x|^2 - 12|x| + 8 & 1 \leq |x| < 2 \\ 0 & 2 \leq |x| \end{cases} \quad (9)$$

This kernel is called the *Parzen window*.